



# HHS Public Access

Author manuscript

*Arch Toxicol.* Author manuscript; available in PMC 2021 December 27.

Published in final edited form as:

*Arch Toxicol.* 2020 June ; 94(6): 1955–1972. doi:10.1007/s00204-020-02729-y.

## Exposure to inorganic arsenic and its methylated metabolites alters metabolomics profiles in INS-1 832/13 insulinoma cells and isolated pancreatic islets

Yuan-Yuan Li<sup>1,2</sup>, Christelle Douillet<sup>2</sup>, Madelyn Huang<sup>3</sup>, Rowan Beck<sup>4</sup>, Susan Jenkins Sumner<sup>1,2</sup>, Miroslav Styblo<sup>2,3</sup>

<sup>1</sup>Nutrition Research Institute, Department of Nutrition, University of North Carolina at Chapel Hill School of Public Health, Chapel Hill, NC 27599, USA

<sup>2</sup>Department of Nutrition, University of North Carolina Gillings School of Global Public Health, Chapel Hill, NC 27599, USA

<sup>3</sup>Curriculum in Toxicology and Environmental Medicine, School of Medicine, University of North Carolina at Chapel Hill, NC 27599, USA (Currently: National Toxicology Program, National Institute of Environmental Health Science, Research Triangle Park, North Carolina)

<sup>4</sup>Curriculum in Genetics and Molecular Biology, School of Medicine, University of North Carolina at Chapel Hill, NC 27599, USA

### Abstract

Inorganic arsenic (iAs) is an environmental diabetogen, but mechanisms underlying its diabetogenic effects are poorly understood. Exposures to arsenite (iAs<sup>III</sup>) and its methylated metabolites, methylarsonite (MAs<sup>III</sup>) and dimethylarsinite (DMAs<sup>III</sup>), have been shown to inhibit glucose stimulated insulin secretion (GSIS) in pancreatic  $\beta$ -cells and isolated pancreatic islets. GSIS is regulated by complex mechanisms. Increase in ATP production through metabolism of glucose and other substrates is the ultimate trigger for GSIS in  $\beta$ -cells. In the present study, we used metabolomics to identify metabolites and pathways perturbed in cultured INS-1 832/13 rat insulinoma cells and isolated murine pancreatic islets by exposures to iAs<sup>III</sup>, MAs<sup>III</sup> and DMAs<sup>III</sup>. We found that the exposures perturbed multiple metabolites, which were enriched primarily in the pathways of amino acid, carbohydrate, phospholipid and carnitine metabolism. However, the effects of arsenicals in INS-1 832/13 cells differed from those in the islets and were exposure specific with very few overlaps between the three arsenicals. In INS-1 832/13 cells, all three arsenicals decreased succinate, a metabolite of Krebs cycle, which provides substrates

Terms of use and reuse: academic research for non-commercial purposes, see here for full terms. <https://www.springer.com/aam-terms-v1>

**Corresponding authors:** Miroslav Styblo, PhD, Department of Nutrition, CB# 74612, University of North Carolina at Chapel Hill, Chapel Hill, NC 27599-7461, USA, Phone: (919) 966-5721, styblo@med.unc.edu Susan Jenkins Sumner, PhD, Nutrition Research Institute, Department of, Nutrition, CB# 74612, Chapel Hill, NC 27599-7461, USA, Phone: 704-250-5066, Susan\_sumner@unc.edu.

#### Conflict of Interest

The authors declare that they have no conflicts of interest.

**Publisher's Disclaimer:** This Author Accepted Manuscript is a PDF file of an unedited peer-reviewed manuscript that has been accepted for publication but has not been copyedited or corrected. The official version of record that is published in the journal is kept up to date and so may therefore differ from this version.

for ATP synthesis in mitochondria. Acetylcarnitine was decreased consistently by exposures to arsenicals in both the cells and the islets. Acetylcarnitine is usually found in equilibrium with Acetyl-CoA, which is the central metabolite in catabolism of macronutrients and the key substrate for Krebs cycle. It is also thought to play an antioxidant function in mitochondria. Thus, while each of the three trivalent arsenicals perturbed specific metabolic pathways, which may or may not be associated with GSIS, all three arsenicals appeared to impair mechanisms that support ATP production or antioxidant defense in mitochondria. These results suggest that impaired ATP production and/or mitochondrial dysfunction caused by oxidative stress may be the mechanisms underlying the inhibition of GSIS in  $\beta$ -cells exposed to trivalent arsenicals.

## Keywords

arsenic; diabetes;  $\beta$ -cells; pancreatic islets; metabolomics

## Introduction

Diabetes is a global health problem. In 2015, the International Diabetes Association estimated that there were 415 million adults with diabetes worldwide and predicted that this number will increase to 642 million in 2040 if the present trends continue (IDF 2015). The US is among the countries with the highest prevalence of diabetes. Approximately 30.3 million US residents (9.4% of the US population) had diabetes in 2017; type 2 diabetes (T2D) accounted for 90–95% of all diabetes cases (CDC 2017). While obesity is recognized as number one cause of T2D, environmental exposures to some of the naturally occurring and synthetic chemicals have also been linked to T2D risk (Auerbach et al. 2016; Bonini and Sargis 2018; Thayer et al. 2012; WHO 2012).

Arsenic (As) is a naturally occurring toxic metalloid (ATSDR 2007). Inorganic As (iAs) has been classified as environmental diabetogen based on overwhelming evidence from multiple cross-sectional and several longitudinal epidemiologic studies (Kuo et al. 2017; Maull et al. 2012; Sung et al. 2015; Wang et al. 2014). Hundreds of millions of people worldwide are exposed to iAs in drinking water (IARC 2004) and even more people consume foods with potentially unsafe levels of iAs (Cubadda et al. 2017). Several mechanisms of the diabetogenic effects of iAs have been suggested by laboratory research, including: (i) inhibition of insulin signaling resulting in insulin resistance in the liver and peripheral tissues and in stimulation of gluconeogenesis, (ii) inhibition of insulin expression and/or secretion in pancreatic  $\beta$ -cells, and (iii) alteration of methylation and/or expression of genes that regulate insulin production, insulin signaling or glucose utilization (Khan et al. 2017; Martin et al. 2017; Maull et al. 2012). However, the contribution of each of these mechanisms to the diabetic phenotype associated with iAs exposure remains unclear.

Over the past several years, work in our laboratory has focused on identification of mechanisms, by which iAs or its metabolites affect  $\beta$ -cell function. We have shown that the trivalent form of iAs (arsenite,  $iAs^{III}$ ) and the mono- and di-methylated trivalent arsenicals ( $MAs^{III}$  and  $DMAs^{III}$ ) that are formed in the course of iAs metabolism, inhibit glucose stimulated insulin secretion in isolated pancreatic islets and in cultured INS-1

832/13 insulinoma cells (Douillet et al. 2013; Dover et al. 2018a; Dover et al. 2018b). Our data suggests that the underlying mechanisms may include: (i) inhibition of mitochondrial metabolism (Dover et al. 2018a), (ii) inhibition of potassium or calcium pumps in plasma membrane (Huang et al. 2019), and (iii) altered expression of microRNAs that have been linked in independent studies to  $\beta$ -cell function (Beck et al. 2017) (Beck et al. 2019). Additional mechanisms have been proposed by other laboratories. For example, Fu and associates showed that exposure of a  $\beta$ -cell line to low concentrations of  $iAs^{III}$  resulted in upregulation of the Nrf2-dependent expression of antioxidant enzymes and subsequent depletion of reactive oxygen species, which are thought to help to stimulate insulin secretion (Fu et al. 2010). Micromolar concentrations of  $iAs^{III}$  have been shown to suppress insulin mRNA expression in primary  $\beta$ -cells (Diaz-Villasenor et al. 2006). Results of a recently published study suggest that  $iAs^{III}$  impaired insulin secretion from pancreatic islets and  $\beta$ -cell function through an ER stress-autophagy pathway (Wu et al. 2018). Another study points to induction of apoptosis through inhibition of thioredoxin reductase activity as the underlying mechanism (Yao et al. 2015). Finally,  $iAs^{III}$  may impair  $\beta$ -cell function and insulin synthesis by suppressing *mafA* expression through activation of microR-149 (Sun et al. 2019).

Thus, the published data suggest that  $iAs^{III}$  can impair  $\beta$ -cell function by targeting multiple steps and pathways involved in the regulation of insulin expression and function or in maintenance of  $\beta$ -cell fitness and viability. It is also likely that the current list of the potential targets is incomplete, and more targets are still to be discovered. Using only  $iAs^{III}$  to study the effects of iAs exposure on  $\beta$ -cell function represents a major limitation of the published studies, because we have shown that  $MAs^{III}$  and  $DMAs^{III}$  are more potent than  $iAs^{III}$  as inhibitors of GSIS and some of the mechanisms regulating this pathway (Dover et al. 2018a) (Douillet et al. 2013). Thus, inclusion of these metabolites or systems that methylate iAs, e.g., isolated pancreatic islets (Douillet et al. 2013), should be an essential requirement for studies aiming to characterize the diabetogenic effects of iAs exposure or to identify the underlying mechanisms.

The goal of the present study was to use metabolomics to (a) characterize metabolic fingerprints of INS-1 832/13 cells and pancreatic islets treated with  $iAs^{III}$ ,  $MAs^{III}$  and  $DMAs^{III}$ , (b) provide a more comprehensive view of the metabolic dysfunction resulting from the interactions of iAs and its metabolites with key pathways in  $\beta$ -cells, and (c) point to targets of arsenic toxicity.

## Methods

### Cell culture and treatment.

INS-1 832/13, rat insulinoma cell line expressing human pro-insulin (Chen et al. 2000; Hohmeier et al. 2000), was a gift from Dr. Newgard (Duke University). The INS-1 832/13 cells were seeded in 12-well tissue culture plates (1 million cells/well) in RPMI 1640 medium (Gibco, Waltham, MA) containing 11 mM glucose and supplemented with 10% FBS, 10 mM HEPES, 2 mM L-glutamine, 1 mM sodium pyruvate, 100 U/ml penicillin, 100  $\mu$ g/ml streptomycin (all from Gibco), and 0.05 mM  $\beta$ -mercaptoethanol (Sigma, St. Louis, MO). The plated cells were cultured at 5%  $CO_2$  and 37°C for 24 hours prior to exposure.

After 24 hours, the supplemented RPMI 1640 medium containing mercaptoethanol was replaced with the same medium lacking mercaptoethanol. The cells were then exposed to 2  $\mu\text{M}$   $\text{iAs}^{\text{III}}$  (sodium arsenite, > 99% pure; Sigma-Aldrich, St. Louis, MO), 0.2  $\mu\text{M}$   $\text{MAs}^{\text{III}}$  (methylarsine oxide, > 98% pure), or 2  $\mu\text{M}$   $\text{DMAs}^{\text{III}}$  (dimethylidoarsine, 98% pure) for 24 hours. INS-1 832/13 cells incubated in the culture medium in absence of arsenicals were used as controls. The methylated trivalent arsenicals were provided by Dr. William Cullen (the University of British Columbia, Canada).

#### **Pancreatic islets and treatment.**

Islets were isolated from pancreata of adult C57BL/J6 male mice as previously described (Douillet et al. 2013). Briefly, the pancreas was perfused and digested with 1 mg/ml collagenase P (Roche Diagnostics Crop, Indianapolis, IN) and islets were purified using a Ficoll PM-400 gradient (GE Healthcare, Chicago, IL). The isolated islets were incubated overnight at 37°C with 5%  $\text{CO}_2$  at 6-well plates in RPMI 1640 medium with 10% fetal bovine serum, 10 mM HEPES, 1 mM sodium pyruvate, 100 U/ml penicillin, and 100  $\mu\text{g}/\text{ml}$  streptomycin (all from Gibco). The islets were then exposed to 2  $\mu\text{M}$   $\text{iAs}^{\text{III}}$ , 0.25  $\mu\text{M}$   $\text{MAs}^{\text{III}}$ , or 0.5  $\mu\text{M}$   $\text{DMAs}^{\text{III}}$  for 48 hours. Control islets were incubated in the culture medium without arsenicals.

#### **GSIS assay in $\beta$ -cells.**

The assay has been previously described in detail (Beck et al. 2019). Briefly, following the 24-hour exposure, the culture medium was replaced with a secretion assay buffer (SAB) comprised of 114 mM NaCl, 4.7 mM KCl, 1.2 mM  $\text{KH}_2\text{PO}_4$ , 1.16 mM  $\text{MgSO}_4$ , 20 mM HEPES, 2.5 mM  $\text{CaCl}_2$ , 0.2% bovine serum albumin, 25.5 mM  $\text{NaHCO}_3$  (all from Sigma-Aldrich), and 0 mM glucose for 40 min. After 40 min in glucose-free medium, INS-1 832/13 cells were incubated in SAB containing 2.5 mM glucose (Sigma-Aldrich) for 60 min and 16.7 mM glucose for 2 hours. The exposures to  $\text{iAs}^{\text{III}}$ ,  $\text{MAs}^{\text{III}}$ , and  $\text{DMAs}^{\text{III}}$  were maintained during all GSIS steps.

#### **GSIS assay in islets.**

The assay has been previously described in detail (Douillet et al. 2013). Briefly, islets exposed to arsenicals or control islets (15 islets/well) were transferred into 12-well culture plates containing a glucose-free buffer (114 mM NaCl, 4.7 mM KCl, 1.2 mM  $\text{KH}_2\text{PO}_4$ , 1.16 mM  $\text{MgSO}_4$ , 20 mM HEPES, 2.5 mM  $\text{CaCl}_2$ , 0.2% bovine serum albumin, and 25.5 mM  $\text{NaHCO}_3$ ; all from Sigma-Aldrich) for 1 h at 37°C and 5%  $\text{CO}_2$ , followed by a 1-hour incubation in the same buffer containing 2.5 mM glucose and a 1-hour incubation in the buffer with 16.7 mM glucose. The exposures to  $\text{iAs}^{\text{III}}$ ,  $\text{MAs}^{\text{III}}$ , and  $\text{DMAs}^{\text{III}}$  continued throughout all GSIS steps.

#### **Insulin analysis.**

The media from each of the incubation steps of the GSIS assays involving INS-1 832/13 cells and islets were collected for insulin analysis. Insulin concentrations were measured using the Ultra Sensitive Mouse Insulin ELISA kit (Crystal Chem USA, Elk Grove Village, IL). Insulin concentration in the media from INS-1 832/13 cells was normalized for the

concentration of cellular protein. The protein concentration was determined after GSIS using the BCA Protein Assay Kit (Abcam, Cambridge, MA).

### UHPLC High Resolution Orbitrap MS Metabolomics

**Sample preparation.**—The metabolomics analysis was carried out in arsenical-treated and control INS-1 832/13 cells and isolated pancreatic islets. Extracts from the cells and the islets were prepared following the published procedures (Spéjel et al. 2013; Lorenz et al. 2011). Briefly, aliquots of frozen cells ( $n=1\times 10^6$ ) or islets ( $n=100$ ) were mixed with 400  $\mu\text{L}$  ice-cold methanol-water (80:20) and homogenized with the Bead Ruptor Elite Bead Mill Homogenizer (OMNI International) at 6.30 m/s for 45 sec in 1 cycle. Supernatants were collected from homogenates after centrifugation at 16,000 rcf for 20 min at 4°C. Quality control pools (QC pool) for INS-1 832/13 cells were prepared by pooling 32- $\mu\text{L}$  supernatant from each of the  $\beta$ -cell samples. Likewise, QC pools for islets were prepared by pooling 32- $\mu\text{L}$  of supernatant from each islet sample. The supernatant (300  $\mu\text{L}$ ) of each study sample and QC pools were dried under Speed-vac. Each dried residue was reconstituted in a 100  $\mu\text{L}$  water-methanol (95:5) mixture containing 500 ng/mL L-tryptophan-d5. A 10- $\mu\text{L}$  aliquot of the reconstituted supernatant was used for the metabolomics analysis.

**Analysis and data acquisition.**—Metabolomics data was acquired on a Vanquish UHPLC system coupled to a Q Exactive™ HF-X Hybrid Quadrupole-Orbitrap Mass Spectrometer (Thermo Fisher Scientific, San Jose, CA). Our UPLC-MS reversed phase platform was established based on the published methods (Zelena et al. 2009; Dunn et al. 2011). Metabolites were separated via an HSS T3 C18 column ( $2.1 \times 100$  mm, 1.7  $\mu\text{m}$ , Waters Corporation) at 50 °C with binary mobile phase of water (A) and methanol (B), each containing 0.1% formic acid (v/v). The UHPLC linear gradient started from 2% B, and increased to 100% B in 16 min, then held for 4 min, with the flow rate at 400  $\mu\text{L}/\text{min}$ . The untargeted data was acquired from 70 to 1050 m/z using the data dependent acquisition mode. Progenesis QI (version 2.1, Waters Corporation) was used for peak picking, alignment, and normalization. Signals that highly varied ( $\text{RSD}>30\%$ ) or that were missing across the QC Pools were excluded for further analysis. Peaks were normalized in Progenesis QI using the “normalize to total intensity” feature.

**Identification and annotation of signals.**—Peaks were identified or annotated by Progenesis QI through matching to an In-house Experimental Standards Library generated by acquiring data for approximately 1000 compounds under identical conditions to study samples, as well as to public database (including HMDB and NIST). Identifications and annotations used available data for retention time (RT), exact mass (MS), MS/MS fragmentation pattern, and isotopic ion pattern. The evidence for identification or annotation of each signal was provided (Table S1 and Table S2). Signals/metabolites reported in the results and discussion section that matched to the in house experimental standards library by (a) RT, MS, and MS/MS are labeled as OL1, or (b) by RT and MS are labeled OL2a. An OL2b label was provided for signals that match by MS and MS/MS to the in-house library, that were outside the retention time tolerance ( $\pm 0.5$  min) for the standards run under identical conditions. Signals matched to public databases are labeled as PDa (MS and

experimental MS/MS), PDb (MS and theoretical MS/MS), and PDc (mass match) are also provided (Table S1 and Table S2).

**Pathway analysis.**—Pathway enrichment analysis was performed by the GeneGo MetaCore™ (Clarivate Analytics, PA) software to identify the perturbed metabolic pathways associated with exposures to arsenicals. Metacore generated the p-value from the hypergeometric test, which represents the enrichment of certain metabolites in a pathway, together with the false discovery rate (FDR). A p-value < 0.05 is indicative of significant enrichment in pathways.

### Statistical Analysis.

The impact of arsenicals on insulin secretion during the GSIS assay were assessed using one-way ANOVAs followed by Tukey multiple-comparison posttests. Differences characterized by  $p < 0.05$  were considered statistically significant. For metabolomics, the normalized data were analyzed by SIMCA 15.0 (Umetrics, Umeå, Sweden) using unsupervised principal component analysis (PCA), and supervised orthogonal partial least squares discriminate analysis (OPLS-DA). Variable Influence on Projections to latent structures (VIP) was calculated by SIMCA 15.0 to determine signals (or metabolites) that differentiate the study groups. In addition, student t-test and fold change (based on mean) for pairwise comparison were calculated by Microsoft excel 2016. The initial analysis was conducted using VIP 1.0 and  $p < 0.05$  for prioritization of signals that differentiated the phenotypic groups for the  $\beta$ -cells, and for the pancreatic islets. Because relatively few signals were important to the differentiation of the pancreatic islets using these criteria, additional analysis of the pancreatic islets was conducting using the criteria of VIP 1.0, or  $p < 0.05$ , or  $|FC| > 2.0$ .

## Results

### Viability of INS-1 832/13 cells and pancreatic islet.

The exposures used in the present study were those that inhibited GSIS or the mechanisms regulating GSIS in our previous, similarly designed experiments (Beck et al. 2019; Beck et al. 2017; Douillet et al. 2013; Dover et al. 2018a). Specifically, INS-1 832/13 cells were exposed to 2  $\mu\text{M}$   $\text{iAs}^{\text{III}}$ , 0.2  $\mu\text{M}$   $\text{MAs}^{\text{III}}$  or 2  $\mu\text{M}$   $\text{DMAs}^{\text{III}}$  for 24 hours; islets were exposed to 2  $\mu\text{M}$   $\text{iAs}^{\text{III}}$ , 0.25  $\mu\text{M}$   $\text{MAs}^{\text{III}}$  or 0.5  $\mu\text{M}$   $\text{DMAs}^{\text{III}}$  for 48 hours. These exposures did not affect viability of isolated pancreatic islets in our published studies (Douillet et al. 2013) or in the present study. However, cytotoxicity was observed in the INS-1 832/13 cells exposed 2  $\mu\text{M}$   $\text{DMAs}^{\text{III}}$  as manifested by ~65% decrease in the cellular protein (i.e., number of cells in the culture). Exposures to 2  $\mu\text{M}$   $\text{iAs}^{\text{III}}$  and 0.2  $\mu\text{M}$   $\text{MAs}^{\text{III}}$  were only marginally cytotoxic, decreasing protein concentrations by 20% (data not shown). To account for cytotoxicity, insulin secretion was normalized for cellular protein of the INS-1 832/13 cells remaining in the culture after GSIS.

### Effects of arsenicals on GSIS.

As expected, insulin secretion increased several folds in both control INS-1 832/13 cells and control islets in response to the stimulation with 16.7 mM glucose (Fig. 1). Exposures



to  $iAs^{III}$  and  $DMAs^{III}$  decreased GSIS in the cells, but only the effect of  $DMAs^{III}$  was statistically significant (Fig. 1a). In contrast, all three arsenicals inhibited significantly GSIS in isolated islets (Fig. 1b).

### Overall effects of arsenicals on the metabolomics profiles in INS-1 832/13 cells and islets.

Unsupervised and supervised multivariate analysis were used to visualize trends among the control and the arsenical-treated INS-1 832/13 cells and pancreatic islets (Fig. 2). A clear distinction between samples derived from the  $DMAs^{III}$ -treated cells and the control cells could be visualized in the unsupervised PCA, indicating that  $DMAs^{III}$  exposure affected the metabolomics profiles of the cells (Fig. 2a). Supervised OPLS-DA of INS-1 832/13 cells (Fig. 2b) also revealed that  $DMAs^{III}$  treatment resulted in metabolic perturbations in the cells, and that other arsenical-treatment groups also differentiate from the control  $\beta$ -cells. No clear differentiation of arsenical-treated pancreatic islets from the control pancreatic islets was observed using the unsupervised PCA (Fig. 2c). OPLS-DA was able to differentiate between the islets treated with  $iAs^{III}$  or  $DMAs^{III}$  and the control islets, but not between  $MAAs^{III}$ -treated and control islets (Fig. 2d).

Supervised OPLS-DA was used to determine the signals most important to differentiation of each arsenical-treatment group from the corresponding control (Fig. 3) for  $\beta$ -cells and for pancreatic islets. The strongest model statistics ( $Q^2 > 0.89$ ) were found for pairwise comparisons of  $\beta$ -cell controls with each arsenical-treatment group (Fig. 3a, b, c). The model statistics ( $Q^2 > 0.68$ ) for the comparison of  $iAs^{III}$ -treated pancreatic islets with control islets (Fig. 3d) also indicated a disruption in metabolism. In contrast, the model statistics ( $Q^2$ ) for  $DMAs^{III}$  versus control (Fig. 3e) and  $MAAs^{III}$  versus control (Fig. 3f) were negative and did not point to significant metabolic perturbations in response to the  $DMAs^{III}$  and  $MAAs^{III}$  treatment in islets.

### Metabolites perturbed in INS-1 832/13 cells and islets by exposure to arsenicals.

The VIP from the OPLS-DA, p-value, and fold change were used to determine which signals were most important to differentiate the control from the arsenical treatment groups.

**INS-1 832/13 cells:** With the criteria of VIP  $\geq 1.0$  and  $p < 0.05$  between the treatment and control groups, the signals differentiating control INS-1 832/13 cells from the INS-1 832/13 cells treated with  $DMAs^{III}$  (456 signals),  $MAAs^{III}$  (109 signals), and  $iAs^{III}$  (46 signals) were prioritized for identification or annotation (Suppl. Table 1a–c) using the in-house physical standards library and public databases.  $DMAs^{III}$  treatment of INS-1 832/13 cells perturbed 37 signals identified by RT, MS, MS/MS (OL1) or RT, MS (OL2a) (Fig. 4a, Table 1), including 15 amino acids (e.g., ornithine, alanine, glutamic acid,  $\gamma$ -Aminobutyric acid, etc.), 11 nucleobases and their derivatives (e.g., cytosine, guanine, hypoxanthine, uridine, etc.), 4 short-chain amides (e.g., spermine, spermidine, serotonin, and nicotinamide), 2 dicarboxylic acid derivatives (e.g. suberic acid and azelaic acid), acetylcarnitine, and phosphorylcholine, as well as reduced glutathione (10.6-fold decrease). In addition, eight nucleobases derivatives were annotated via matching with MS/MS spectra from either in-house library or public database (i.e, OL2b or PDA, Suppl. Table 1). Compared to  $DMAs^{III}$ ,  $MAAs^{III}$  and  $iAs^{III}$  had relatively less impact on the metabolic profiles of INS-1

832/13 cells (Fig. 4a, Table 1). Nine metabolites (OL1 and OL2a) were significantly ( $p < 0.05$ ) perturbed by  $\text{MAs}^{\text{III}}$  and 5 by  $\text{iAs}^{\text{III}}$ . Two metabolites, acetylcarnitine and succinic acid, were decreased (1.4- to 1.8-fold) following exposure to each of the three arsenicals. Aminobutyric acid and nicotinamide were significantly decreased after exposure to  $\text{iAs}^{\text{III}}$  and  $\text{DMAs}^{\text{III}}$ , but not after exposure to  $\text{MAs}^{\text{III}}$ . N-methyl-L-glutamic acid and glutamic acids were decreased after exposure to  $\text{MAs}^{\text{III}}$  and  $\text{DMAs}^{\text{III}}$ , but not after exposure to  $\text{iAs}^{\text{III}}$ . Five metabolites (cyclic adenosine monophosphate, carnitine, aspartic acid, raffinose, and O-phosphorylethanolamine) were perturbed only following exposure to  $\text{MAs}^{\text{III}}$ .

**Pancreatic Islets:** The overall impact of arsenical exposures on islet cells was less than that found in  $\beta$ -cells. Using the same criteria of  $\text{VIP} \geq 1$  and  $p < 0.05$  that was used in the INS-1 832/13 cells analysis, few signals were identified or annotated that differentiated the study groups (Fig. 4b). We found that three metabolites, including methylthioadenosine (OL1), undecanedicarboxylic acid (PDc), and glutamylisoleucine (PDd) were decreased in the  $\text{MAs}^{\text{III}}$  treated islets compared to the control islets. A sulfonic acid derivative (PDd) was decreased in the  $\text{DMAs}^{\text{III}}$  treated islets compared to the control islets; and one metabolite, angiotensin I (PDd) was decreased in the  $\text{iAs}^{\text{III}}$  treated islets versus control islets. A common signal that was perturbed amongst three arsenicals treatments or between any of the two arsenical treatments could not be identified or annotated. To gain more information regarding signals/metabolites differentiating the arsenical-treated islets from the islets control, criteria were set to  $\text{VIP} \geq 1.0$ , or  $p < 0.05$ , or  $|\text{FC}| > 2.0$ . Using these less stringent criteria, signals differentiating control islets from islets treated with  $\text{iAs}^{\text{III}}$  (83 signals),  $\text{DMAs}^{\text{III}}$  (75 signals) and  $\text{MAs}^{\text{III}}$  (65 signals) were prioritized for identification and annotation (Suppl. Table 2a–c) via in-house experimental library and public database. Amongst these signals/metabolites, 29 of them were identified with OL1 or OL2a level, including 12 perturbed by  $\text{DMAs}^{\text{III}}$ , 14 perturbed by  $\text{MAs}^{\text{III}}$ , and 15 perturbed by  $\text{iAs}^{\text{III}}$  (Fig. 4c, Table 2). In general, the fold-change level of metabolites associated with the arsenical exposures in the isolated pancreatic islets were not as pronounced as those found in  $\beta$ -cells, with the greatest change (3.9-fold) found for hypotaurine in the islets exposed to  $\text{iAs}^{\text{III}}$ . Two fatty acid derivatives, suberic acid and petroselinic acid had  $\text{VIP} > 1.0$  for all three exposures versus control. Two metabolites decreased following exposure to both  $\text{iAs}^{\text{III}}$  and  $\text{MAs}^{\text{III}}$  - glutamic acid and S-adenosylmethionine (which is required for methylation of arsenic). Some perturbations were uniquely associated with exposure to a specific arsenical. In particular, sucrose, hypotaurine and sorbitol were increased after exposure to  $\text{iAs}^{\text{III}}$ . Methylthioadenosine, betaine and lysine were decreased after exposure to  $\text{MAs}^{\text{III}}$ . The reduced form of glutathione was decreased after exposure to  $\text{DMAs}^{\text{III}}$ .

### Pathways enriched with the altered metabolites.

GeneGo Metcore was used to enrich the metabolic pathways perturbed by arsenical treatments based on the identified metabolites (OL1 or OL2a) differentiating the arsenical treated group from control in INS-1 832/13 cells and in the isolated pancreatic islets, respectively. The analysis used a cut-off for the significance of the pathway enrichment at  $p < 0.05$  (Table 3 and 4). In  $\beta$ -cells, 25 and 17 metabolic pathways were enriched by exposures to  $\text{DMAs}^{\text{III}}$  and  $\text{MAs}^{\text{III}}$ , respectively; as compared to only 6 pathways enriched by exposure to  $\text{iAs}^{\text{III}}$  (Fig. 5a, Table 3). The exposure to  $\text{DMAs}^{\text{III}}$  was associated with



perturbation (mostly downregulation) of multiple pathways of amino acid transport and metabolism. Some of the same pathways were also downregulated by  $\text{MAs}^{\text{III}}$  exposure. The D-glucuronic acid pathways was the only pathway downregulated by all three arsenicals. Fourteen pathways were uniquely perturbed by  $\text{DMAs}^{\text{III}}$  and 4 by  $\text{MAs}^{\text{III}}$  exposures; none of the affected pathways was associated only with exposure to  $\text{iAs}^{\text{III}}$ . Three pathways of carbohydrate metabolism, including TCA cycle and propionate metabolism, as well as the L-carnitine pathway were downregulated by  $\text{iAs}^{\text{III}}$  and  $\text{MAs}^{\text{III}}$ , but not by  $\text{DMAs}^{\text{III}}$ . Similarly, the pathways of amino acid (Ala, Ser, Cys, Met, His, Pro, Gly, Glu, Gln) metabolism and glycosphingolipid metabolism were affected (downregulated) by  $\text{iAs}^{\text{III}}$  and  $\text{DMAs}^{\text{III}}$ , but not by  $\text{MAs}^{\text{III}}$ .

Unlike in  $\beta$ -cells, most of the enriched pathways in the isolated pancreatic islets (21) were associated with the exposure to  $\text{iAs}^{\text{III}}$ ; 17 of these pathways were unique to  $\text{iAs}^{\text{III}}$  exposure and included pathways of amino acid, glycerol-3-phosphocholine and carbohydrate metabolism (Fig. 5b, Table 4). In comparison, 16 pathways were perturbed by exposure to  $\text{MAs}^{\text{III}}$  and 6 of them were unique to  $\text{MAs}^{\text{III}}$ ; while 12 pathways were perturbed by exposure to  $\text{DMAs}^{\text{III}}$  and 3 of them were unique to  $\text{DMAs}^{\text{III}}$ . The exposures to  $\text{MAs}^{\text{III}}$  and  $\text{DMAs}^{\text{III}}$  affected multiple pathways of amino acid metabolism, some of which were unique to  $\text{MAs}^{\text{III}}$  exposure (e.g., pathways of lysine, glutamic acid and methionine metabolism) and some to  $\text{DMAs}^{\text{III}}$  exposure (e.g., pathways of tyrosine and (S)-citrulline metabolism). There was no overlap between the three exposures, i.e., no pathway was affected by exposure to all of the three arsenicals. In general, the pathways enriched in islets showed lower significance in enrichment [-log (p-value)] with higher false discovery rate, compared to the results in  $\beta$ -cells.

### **Effects of arsenicals on metabolites in the pathways of carbohydrate, amino acid and carnitine metabolism.**

The pathways of carbohydrate and amino acid metabolism were among the pathways most affected by the exposures to arsenicals in both the INS-1 832/13 cells and the islets. To better understand the extent and directions of these effects, we compared the relative intensities of key metabolites among the three exposures focusing on  $\beta$ -cells. Consistent with results obtained from Genego Metacore, we found that the arsenicals lowered two metabolites shared by glycolysis and gluconeogenesis (fructose-1,6-bis-phosphate and lactate), as well as two metabolites in Krebs cycle (succinate, and fumarate) (Fig 6; Suppl. Fig. 1). In addition, all 3 arsenicals significantly reduced glutamate (glutamic acid), while individual arsenicals reduced other glucogenic and ketogenic amino acids that provide carbons to Krebs cycle or can be synthesized using Krebs cycle metabolites. Most of these amino acids were lowered by exposure to  $\text{DMAs}^{\text{III}}$  while the impacts of  $\text{iAs}^{\text{III}}$  and  $\text{MAs}^{\text{III}}$  were relatively minor.

Carnitine and its derivatives were also significantly altered in INS-1 832/13 cells exposed to arsenicals, but here the directions of the effects differed (Suppl. Fig. 2). The exposures to  $\text{iAs}^{\text{III}}$  and  $\text{MAs}^{\text{III}}$  significantly increased while  $\text{DMAs}^{\text{III}}$  lowered carnitine level. We also noticed that the precursor of carnitine synthesis, deoxycarnitine, were lower by  $\text{DMAs}$  but not influenced by either  $\text{iAs}^{\text{III}}$  or  $\text{MAs}^{\text{III}}$ . In contrast, acetylcarnitine levels were lowered

by all these arsenicals. Short-chain acyl carnitines were perturbed mainly by exposure to DMAs<sup>III</sup>. DMAs<sup>III</sup> significantly lowered valerylcarnitine (C5) and glutarylcarnitine (C5-DC), while increasing butenylcarnitine (C4:1) levels. The exposures to arsenical also altered middle- and long-chain acylcarnitines. Specifically, iAs<sup>III</sup> increased palmitoylcarnitine (C16) and octanoylcarnitine (C8), while DMAs<sup>III</sup> increased dodecanedioylcarnitine (C12-DC).

### Metabolites perturbed by arsenicals in both INS-1 832/13 cells and islets.

Comparison of the metabolites that were altered by arsenicals in INS-1 832/13 cells and in islets revealed 13 overlapping metabolites (Fig. 7, Table 5). Among those metabolites was acetylcarnitine, which was decreased in the islets exposed to MAs<sup>III</sup> and DMAs<sup>III</sup> and in INS-1 832/13 cells exposed to iAs<sup>III</sup>, MAs<sup>III</sup> or DMAs<sup>III</sup>. Exposure to MAs<sup>III</sup> increased glutamate levels in the cells and glutamate was also among the metabolites altered in islets exposed to iAs<sup>III</sup>. Suberic acid was altered in the islets exposed to any of the three arsenicals, as well as in the cells exposed to DMAs<sup>III</sup>. Several metabolites altered by DMAs<sup>III</sup> in the cells, including hypoxanthine, methylthioadenosine and amino acids leucine and valine, were also altered in the islets exposed to iAs<sup>III</sup>. Finally, DMAs<sup>III</sup> exposure decreased reduced glutathione and ornithine levels in both the cells and the islets. In general, the impacts of the exposures on the overlapping metabolites in the cells were greater than in the islets (based on the fold change).

## Discussion

We have previously reported that iAs<sup>III</sup> and its trivalent methylated metabolites, MAs<sup>III</sup> and DMAs<sup>III</sup>, inhibit GSIS in isolated pancreatic islets (Douillet et al. 2013). We have also shown that exposures to iAs<sup>III</sup> and MAs<sup>III</sup> impair energy metabolism in mitochondria of INS-1 832/13 cells (Dover et al. 2018a), which is an important factor regulating insulin secretion in response to glucose challenge (Rorsman et al. 2000). The main goal of the present study was to identify metabolic pathways and specific metabolites in INS-1 832/13 cells and pancreatic islets that are altered by exposures to trivalent arsenicals and which may be linked to the impaired GSIS. We used the exposure windows and the concentrations of iAs<sup>III</sup>, MAs<sup>III</sup> and DMAs<sup>III</sup>, which in previous studies significantly inhibited GSIS but had no effects on viability of INS-1 832/13 cells or isolated islets. However, unlike in the previous studies, mercaptoethanol, which is required for maintenance and expansion of INS-1 832/13 cells (Chen et al. 2000; Hohmeier et al. 2000), was omitted from the culture medium for the time of the exposure to avoid interactions between the thiol group of mercaptoethanol and arsenicals. Under these conditions, DMAs<sup>III</sup> significantly inhibited GSIS and was cytotoxic for  $\beta$ -cells. This suggests that the presence of mercaptoethanol, and possibly other thiols in the medium, may alter effects of trivalent arsenicals in this type of cells. Notably, the effects of the trivalent arsenicals on GSIS and viability of isolated pancreatic islets were consistent with results our previously published study (Douillet et al. 2013).

Results of the metabolomics analyses suggest that the numbers of metabolites and pathways disrupted by exposures to arsenicals correlate with their effects on GSIS. In  $\beta$ -cells, exposure to DMAs<sup>III</sup>, the only arsenical that inhibited GSIS, induced much greater

perturbations in metabolomics profiles than exposure to either  $iAs^{III}$  or  $MAs^{III}$ . In the islets,  $iAs^{III}$ , which appeared to be the most potent inhibitor of GSIS, disturbed more metabolites and pathways than either  $MAs^{III}$  or  $DMAs^{III}$ . In general, exposures to arsenicals had greater impacts on metabolic profiles in INS-1 832/13 cells than in islets. This could be explained by differences in the  $\beta$ -cell and islet morphology and the fact that islets consist of several structurally and functionally different cell types (Folli et al. 2018), which may differ in their responses to arsenic exposure. In addition, unlike the INS-1 832/13  $\beta$ -cells, isolated murine pancreatic islets methylate  $iAs^{III}$  and  $MAs^{III}$  (Douillet et al. 2013). Thus, the metabolic disturbances we observed in the islets exposed to  $iAs^{III}$  are results of the exposure to a mixture of tri- and pentavalent  $iAs$ ,  $MAs$  and  $DMAs$ , which are formed in the course of  $iAs^{III}$  metabolism. Similarly, exposure of islets to  $MAs^{III}$  would result in a mixture of tri- and pentavalent  $MAs$  and  $DMAs$ . Thus, while isolated islets provide a more physiological model to study metabolomics of arsenic exposure than the INS-1 832/13  $\beta$ -cell line, the interpretation of results is complicated by the complexity of this model.

Most of the effects on metabolomics profiles in both INS-1 832/13 cells and islets were exposure-specific. In  $\beta$ -cells, exposure to  $DMAs^{III}$  perturbed a wide spectrum of metabolites that enriched fourteen  $DMAs^{III}$ -specific pathways, mainly pathways of amino acid metabolism and transport. In contrast, all four pathways uniquely altered by  $MAs^{III}$  exposure involved various forms of acyl-carnitine, which functions as a mechanism for transport of fatty acids from cytoplasm to mitochondrial matrix for  $\beta$ -oxidation and energy production. In the islets, nineteen pathways were uniquely perturbed by exposure to  $iAs^{III}$ . The majority of these pathways were linked to carbohydrate and phospholipid (phosphocholine) metabolism. In comparison, the pathways uniquely disrupted by exposures to  $MAs^{III}$  or  $iAs^{III}$  were all associated with metabolism of amino acids. These findings suggest that in spite of their similar chemical properties, specifically the presence of trivalent arsenic in their molecular structures,  $iAs^{III}$ ,  $MAs^{III}$  and  $DMAs^{III}$  target different metabolic pathways in INS-1 832/13 cells and pancreatic islets, and thus may impair GSIS through different mechanisms.

We found relatively minor overlaps between metabolites and pathways that were disrupted by exposure to  $iAs^{III}$ ,  $MAs^{III}$  and  $DMAs^{III}$ . In  $\beta$ -cells, only two metabolites, succinic acid and acetylcarnitine, were altered (both decreased) by each of the three arsenicals. Succinate is a key metabolite of Krebs cycle, a mitochondrial pathway that oxidizes carbons from all major macronutrients to  $CO_2$ . More importantly, it provides substrates for electron transport chain in the inner mitochondrial membrane, which is coupled to oxidative phosphorylation, the major pathway for ATP synthesis in mammalian cells. The formation of ATP in the course of glucose oxidation and increase in ATP/ADP ratio is one of the trigger mechanisms for insulin secretion in  $\beta$ -cells (Rorsman et al. 2000). Acetylcarnitine, a product of the reaction of acetyl-CoA with carnitine in mitochondria (Farrell et al. 1986), has been shown to stimulate insulin secretion from  $\beta$ -cells (Aichler et al. 2017). In addition, treatment with acetylcarnitine improved mitochondrial respiration (Iossa et al. 2002) and reversed type 1 diabetes phenotype in laboratory mice treated with streptozotocin (Cresto et al. 2006). Thus, the downregulation of these two metabolites in INS-1 832/13 cells exposed to the arsenicals is consistent with  $\beta$ -cell dysfunction. Only one pathway, the D-glucuronic acid pathway, was found to be altered (downregulated) in INS-1 832/13 cells after exposure to any of the

three arsenicals. D-glucuronic acid is formed by oxidation of carbon-6 of glucose mainly in the liver and facilitates transport of various endogenous and exogenous compounds around the body (Mano et al. 2018; Yang et al. 2017). It also functions as a building block of proteoglycans and glycolipids (Esko et al. 2009; Meng et al. 2019). However, there are no published data to directly link this pathway either to iAs exposure or to  $\beta$ -cell function.

Thirteen metabolites were perturbed by exposures to arsenicals in both INS-1 832/13 cells and islets, but the direction and magnitude of the changes differed and were exposure specific. Acetylcarnitine was the most consistently altered metabolite. A decrease in acetylcarnitine was observed in the INS-1 832/13 cells exposed to all three arsenicals, as well as in the islets exposed to  $\text{MAs}^{\text{III}}$  and  $\text{DMAs}^{\text{III}}$ . Endogenous acetylcarnitine is found in equilibrium with acetyl-CoA, the key product of catabolism of carbohydrates, amino acids and fatty acids, and the substrate for Krebs cycle (Rosca et al. 2009) Lower levels of acetylcarnitine would indicate low acetyl-CoA production, and consequently an impaired production of ATP in mitochondria. Acetylcarnitine is also thought to play an antioxidant function (Calabrese et al. 2006). Treatment with acetylcarnitine has been shown to attenuate tissue injury in rats exposed to  $\text{iAs}^{\text{III}}$  by reversing iAs-induced oxidative stress, inflammation and mitochondrial dysfunction (Bodaghi-Namileh et al. 2018; Keshavarz-Bahaghighat et al. 2018; Sepand et al. 2016). Thus, it is possible that the decrease in acetylcarnitine in both INS-1 832/13 cells and islets exposed to the trivalent arsenicals was in response to oxidative stress induced by these arsenicals. Our finding that the exposure to  $\text{DMAs}^{\text{III}}$  decreased reduced glutathione, the major intracellular antioxidant, in both INS-1 832/13 cells (10.6 times) and islets (2.1 times) supports this hypothesis.

The present study used two well-established *in vitro* models for diabetes research, INS-1 832/13  $\beta$ -cells and isolated murine pancreatic islets. Unlike most previously published studies that focused only on  $\text{iAs}^{\text{III}}$ , we examined effects of all three trivalent arsenicals that are associated with iAs exposure ( $\text{iAs}^{\text{III}}$ ,  $\text{MAs}^{\text{III}}$  and  $\text{DMAs}^{\text{III}}$ ) and are thought to be jointly responsible for adverse phenotypes associated with this exposure, including diabetes. We have used the cutting-edge untargeted metabolomics to reveal metabolic profiles and pathways that were perturbed in response to these trivalent arsenicals in both *in vitro* models. These are undisputable strengths of the present study. On the other hand, using only one dose and one exposure window for each arsenical in each cell culture model may represent a significant limitation; however, using multiple doses or exposure times was cost-prohibitive for this study. In this study, unlike in our previous studies,  $\text{iAs}^{\text{III}}$  and  $\text{MAs}^{\text{III}}$  did not inhibit GSIS in INS-1 832/13 cells, possibly because of the absence of mercaptoethanol in the culture medium. This makes it difficult to link the observed metabolic perturbations directly to  $\beta$ -cell dysfunction. Still, these perturbations may represent early events that could lead to impaired GSIS in  $\beta$ -cells exposed to these arsenicals.

## Conclusions

Results of the present study suggest that exposure of pancreatic islets, and specifically  $\beta$ -cells to iAs or the methylated trivalent arsenicals that are formed in the course of iAs metabolism results in significant perturbations of multiple metabolites and metabolic

pathways, including pathways of amino acid, carbohydrate, carnitine and phospholipid metabolism. Perturbations in some of these pathways, e.g., those involved in energy metabolism or antioxidant defense in mitochondria, may be responsible for the impaired  $\beta$ -cell function as a potential mechanism of diabetes associated with iAs exposure. Notably, iAs<sup>III</sup>, MAs<sup>III</sup> and DMAs<sup>III</sup> appear to target different metabolic pathways, suggesting that the efficiency of iAs methylation and the distribution of arsenic metabolites in the pancreas and within the pancreatic islets may play critical role in the impairment of  $\beta$ -cell function and in the development of diabetes in individuals exposed to iAs.

## Supplementary Material

Refer to Web version on PubMed Central for supplementary material.

## Acknowledgements

This study was supported by the NIEHS grant R01ES022697 (PI, Styblo), the UNC Nutrition Obesity Research Center grant DK056350 from NIDDK (PI, Zeisel), and the NIH Common Fund Grant 1U24DK097193 (Sumner, PI). All raw and normalized analytical data and associated metadata have been uploaded to the publicly accessible NIH Common Fund Metabolomics Data Repository (doi: 0.21228/M8PH4S; Project ID: PR000851). We thank Dr. Wimal Pathmasiri for assistance with the pathway analysis.

## REFERENCES

- Aichler M, Borgmann D, Krumsiek J, Buck A, MacDonald PE, Fox JEM, Lyon J, Light PE, Keipert S, Jastroch M, Feuchtinger A, Mueller NS, Sun N, Palmer A, Alexandrov T, Hrabe de Angelis M, Neschen S, Tschop MH, Walch A (2017) N-acyl Taurines and Acylcarnitines Cause an Imbalance in Insulin Synthesis and Secretion Provoking beta Cell Dysfunction in Type 2 Diabetes. *Cell Metab* 25(6):1334–1347 e4 [PubMed: 28591636]
- ATSDR (2007) Toxicological profile for arsenic. U.S. DHHS, Public Health Service, Agency for Toxic Substances and Disease Registry
- Auerbach S, Filer D, Reif D, Walker V, Holloway AC, Schlezinger J, Srinivasan S, Svoboda D, Judson R, Bucher JR, Thayer KA (2016) Prioritizing Environmental Chemicals for Obesity and Diabetes Outcomes Research: A Screening Approach Using ToxCast High-Throughput Data. *Environ Health Perspect* 124(8):1141–54 [PubMed: 26978842]
- Beck R, Chandi M, Kanke M, Styblo M, Sethupathy P (2019) Arsenic is more potent than cadmium or manganese in disrupting the INS-1 beta cell microRNA landscape. *Arch Toxicol* 93(11):3099–3109 [PubMed: 31555879]
- Beck R, Styblo M, Sethupathy P (2017) Arsenic Exposure and Type 2 Diabetes: MicroRNAs as Mechanistic Links? *Curr Diab Rep* 17(3):18 [PubMed: 28275977]
- Bodaghi-Namileh V, Sepand MR, Omidi A, Aghsami M, Seyednejad SA, Kasirzadeh S, Sabzevari O (2018) Acetyl-L-carnitine attenuates arsenic-induced liver injury by abrogation of mitochondrial dysfunction, inflammation, and apoptosis in rats. *Environ Toxicol Pharmacol* 58:11–20 [PubMed: 29278859]
- Bonini MG, Sargis RM (2018) Environmental Toxicant Exposures and Type 2 Diabetes Mellitus: Two Interrelated Public Health Problems on the Rise. *Curr Opin Toxicol* 7:52–59 [PubMed: 29392186]
- Calabrese V, Giuffrida Stella AM, Calvani M, Butterfield DA (2006) Acetylcarnitine and cellular stress response: roles in nutritional redox homeostasis and regulation of longevity genes. *J Nutr Biochem* 17(2):73–88 [PubMed: 16413418]
- CDC (2017) National Diabetes Statistics Report, 2017. Estimates of Diabetes and Its Burden in the United States. National Center for Chronic Disease Prevention and Health Promotion, Division of Diabetes Translation

- Chen G, Hohmeier HE, Gasa R, Tran VV, Newgard CB (2000) Selection of insulinoma cell lines with resistance to interleukin-1 $\beta$ - and gamma-interferon-induced cytotoxicity. *Diabetes* 49(4):562–70 [PubMed: 10871193]
- Cresto JC, Fabiano de Bruno LE, Cao GF, Pastorale CF, Confalonieri N, del Carmen Camberos M, Basabe JC (2006) The association of acetyl-L-carnitine and nicotinamide remits the experimental diabetes in mice by multiple low-dose streptozotocin. *Pancreas* 33(4):403–11 [PubMed: 17079947]
- Cubadda F, Jackson BP, Cottingham KL, Van Horne YO, Kurzius-Spencer M (2017) Human exposure to dietary inorganic arsenic and other arsenic species: State of knowledge, gaps and uncertainties. *Sci Total Environ* 579:1228–1239 [PubMed: 27914647]
- Diaz-Villasenor A, Sanchez-Soto MC, Cebrian ME, Ostrosky-Wegman P, Hiriart M (2006) Sodium arsenite impairs insulin secretion and transcription in pancreatic  $\beta$ s. *Toxicol Appl Pharmacol* 214(1):30–4 [PubMed: 16413591]
- Douillet C, Currier J, Saunders J, Bodnar WM, Matousek T, Styblo M (2013) Methylated trivalent arsenicals are potent inhibitors of glucose stimulated insulin secretion by murine pancreatic islets. *Toxicol Appl Pharmacol* 267(1):11–5 [PubMed: 23261974]
- Dover EN, Beck R, Huang MC, Douillet C, Wang Z, Klett EL, Styblo M (2018a) Arsenite and methylarsonite inhibit mitochondrial metabolism and glucose-stimulated insulin secretion in INS-1 832/13 beta cells. *Arch Toxicol* 92(2):693–704 [PubMed: 28956099]
- Dover EN, Patel NY, Styblo M (2018b) Impact of in vitro heavy metal exposure on pancreatic beta-cell function. *Toxicol Lett* 299:137–144 [PubMed: 30300733]
- Dunn WB, Broadhurst D, Begley P, Zelena E, Francis-McIntyre S, Anderson N, Brown M, Knowles JD, Halsall A, Haselden JN, Nicholls AW (2011) Procedures for large-scale metabolic profiling of serum and plasma using gas chromatography and liquid chromatography coupled to mass spectrometry. *Nature protocols* 6(7): 1060–1083 [PubMed: 21720319]
- Esko JD, Kimata K, Lindahl U (2009) Proteoglycans and Sulfated Glycosaminoglycans. In: nd, Varki A, Cummings RD, et al. (eds) *Essentials of Glycobiology*. Cold Spring Harbor (NY)
- Farrell S, Vogel J, Bieber LL (1986) Entry of acetyl-L-carnitine into biosynthetic pathways. *Biochim Biophys Acta* 876(1):175–7 [PubMed: 3081044]
- Folli F, La Rosa S, Finzi G, Davalli AM, Galli A, Dick EJ Jr., Perego C, Mendoza RG (2018) Pancreatic islet of Langerhans' cytoarchitecture and ultrastructure in normal glucose tolerance and in type 2 diabetes mellitus. *Diabetes Obes Metab* 20 Suppl 2:137–144 [PubMed: 30230173]
- Fu J, Woods CG, Yehuda-Shnaidman E, Zhang Q, Wong V, Collins S, Sun G, Andersen ME, Pi J (2010) Low-level arsenic impairs glucose-stimulated insulin secretion in pancreatic beta cells: involvement of cellular adaptive response to oxidative stress. *Environ Health Perspect* 118(6):864–70 [PubMed: 20100676]
- Hohmeier HE, Mulder H, Chen G, Henkel-Rieger R, Prentki M, Newgard CB (2000) Isolation of INS-1-derived cell lines with robust ATP-sensitive K<sup>+</sup> channel-dependent and independent glucose-stimulated insulin secretion. *Diabetes* 49(3):424–30 [PubMed: 10868964]
- Huang M, Douillet C, Styblo M (2019) Arsenite and its trivalent methylated metabolites inhibit glucose-stimulated calcium influx and insulin secretion in murine pancreatic islets. *Arch Toxicol* 93(9):2525–2533 [PubMed: 31332465]
- IARC (2004) *Some Drinking-water Disinfectants and Contaminants, including Arsenic.*, vol 84. WHO, International Agency for Research of Cancer, Geneva, Switzerland
- IDF (2015) *IDF Diabetes Atlas, 7th Edition*, [www.diabetesatlas.org](http://www.diabetesatlas.org) edn. International Diabetes Federation
- Iossa S, Mollica MP, Lionetti L, Crescenzo R, Botta M, Barletta A, Liverini G (2002) Acetyl-L-carnitine supplementation differently influences nutrient partitioning, serum leptin concentration and skeletal muscle mitochondrial respiration in young and old rats. *J Nutr* 132(4):636–42 [PubMed: 11925454]
- Keshavarz-Bahaghighat H, Sepand MR, Ghahremani MH, Aghsami M, Sanadgol N, Omidi A, Bodaghi-Namileh V, Sabzevari O (2018) Acetyl-L-Carnitine Attenuates Arsenic-Induced Oxidative Stress and Hippocampal Mitochondrial Dysfunction. *Biol Trace Elem Res* 184(2):422–435 [PubMed: 29189995]



- Khan F, Momtaz S, Niaz K, Hassan FI, Abdollahi M (2017) Epigenetic mechanisms underlying the toxic effects associated with arsenic exposure and the development of diabetes. *Food Chem Toxicol* 107(Pt A):406–417 [PubMed: 28709971]
- Kuo CC, Moon KA, Wang SL, Silbergeld E, Navas-Acien A (2017) The Association of Arsenic Metabolism with Cancer, Cardiovascular Disease, and Diabetes: A Systematic Review of the Epidemiological Evidence. *Environ Health Perspect* 125(8):087001 [PubMed: 28796632]
- Lorenz MA, Burant CF, Kennedy RT (2011) Reducing time and increasing sensitivity in sample preparation for adherent mammalian cell metabolomics: *Analytical chemistry* 83(9): 3406–3414. [PubMed: 21456517]
- Mano ECC, Scott AL, Honorio KM (2018) UDP-glucuronosyltransferases: Structure, Function and Drug Design Studies. *Curr Med Chem* 25(27):3247–3255 [PubMed: 29484974]
- Martin EM, Styblo M, Fry RC (2017) Genetic and epigenetic mechanisms underlying arsenic-associated diabetes mellitus: a perspective of the current evidence. *Epigenomics* 9(5):701–710 [PubMed: 28470093]
- Maull EA, Ahsan H, Edwards J, Longnecker MP, Navas-Acien A, Pi J, Silbergeld EK, Styblo M, Tseng CH, Thayer KA, Loomis D (2012) Evaluation of the association between arsenic and diabetes: a National Toxicology Program workshop review. *Environ Health Perspect* 120(12):1658–70 [PubMed: 22889723]
- Meng DH, Du RR, Chen LZ, Li MT, Liu F, Hou J, Shi YK, Wang FS, Sheng JZ (2019) Cascade synthesis of uridine-5'-diphosphate glucuronic acid by coupling multiple whole cells expressing hyperthermophilic enzymes. *Microb Cell Fact* 18(1):118 [PubMed: 31262296]
- Rorsman P, Eliasson L, Renstrom E, Gromada J, Barg S, Gopel S (2000) The Cell Physiology of Biphasic Insulin Secretion. *News Physiol Sci* 15:72–77 [PubMed: 11390882]
- Rosca MG, Lemieux H, Hoppel CL (2009) Mitochondria in the elderly: Is acetylcarnitine a rejuvenator? *Adv Drug Deliv Rev* 61(14):1332–1342 [PubMed: 19720100]
- Seband MR, Razavi-Azarkhiavi K, Omidi A, Zirak MR, Sabzevari S, Kazemi AR, Sabzevari O (2016) Effect of Acetyl-L-Carnitine on Antioxidant Status, Lipid Peroxidation, and Oxidative Damage of Arsenic in Rat. *Biol Trace Elem Res* 171(1):107–15 [PubMed: 26349760]
- Spégl P, Sharoyko VV, Goehring I, Danielsson AP, Malmgren S, Nagorny CL, Andersson LE, Koeck T, Sharp GW, Straub SG, Wollheim CB, Mulder H (2013) Time-resolved metabolomics analysis of beta-cells implicates the pentose phosphate pathway in the control of insulin release. *Biochem J* 450(3):595–605 [PubMed: 23282133]
- Sun Q, Yang Q, Xu H, Xue J, Chen C, Yang X, Gao X, Liu Q (2019) miR-149 Negative Regulation of mafA Is Involved in the Arsenite-Induced Dysfunction of Insulin Synthesis and Secretion in Pancreatic Beta Cells. *Toxicol Sci* 167(1):116–125 [PubMed: 29905828]
- Sung TC, Huang JW, Guo HR (2015) Association between Arsenic Exposure and Diabetes: A Meta-Analysis. *Biomed Res Int* 2015:368087 [PubMed: 26000288]
- Thayer KA, Heindel JJ, Bucher JR, Gallo MA (2012) Role of environmental chemicals in diabetes and obesity: a National Toxicology Program workshop review. *Environ Health Perspect* 120(6):779–89 [PubMed: 22296744]
- Wang W, Xie Z, Lin Y, Zhang D (2014) Association of inorganic arsenic exposure with type 2 diabetes mellitus: a meta-analysis. *J Epidemiol Community Health* 68(2):176–84 [PubMed: 24133074]
- WHO (2012) State of the Science of Endocrine Disrupting Chemicals - 2012. WHO, Geneva, Switzerland
- Wu W, Yao X, Jiang L, Zhang Q, Bai J, Qiu T, Yang L, Gao N, Yang G, Liu X, Chen M, Sun X (2018) Pancreatic islet-autonomous effect of arsenic on insulin secretion through endoplasmic reticulum stress-autophagy pathway. *Food Chem Toxicol* 111:19–26 [PubMed: 29111283]
- Yang N, Sun R, Liao X, Aa J, Wang G (2017) UDP-glucuronosyltransferases (UGTs) and their related metabolic cross-talk with internal homeostasis: A systematic review of UGT isoforms for precision medicine. *Pharmacol Res* 121:169–183 [PubMed: 28479371]
- Yao XF, Zheng BL, Bai J, Jiang LP, Zheng Y, Qi BX, Geng CY, Zhong LF, Yang G, Chen M, Liu XF, Sun XC (2015) Low-level sodium arsenite induces apoptosis through inhibiting TrxR activity in pancreatic beta-cells. *Environ Toxicol Pharmacol* 40(2):486–91 [PubMed: 26291581]

Zelena E, Dunn WB, Broadhurst D, Francis-McIntyre S, Carroll KM, Begley P, O'Hagan S, Knowles JD, Halsall A, HUSERMET Consortium, Wilson ID (2009) Development of a robust and repeatable UPLC– MS method for the long-term metabolomic study of human serum. *Analytical chemistry* 81(4):1357–1364 [PubMed: 19170513]

Author Manuscript

Author Manuscript

Author Manuscript

Author Manuscript

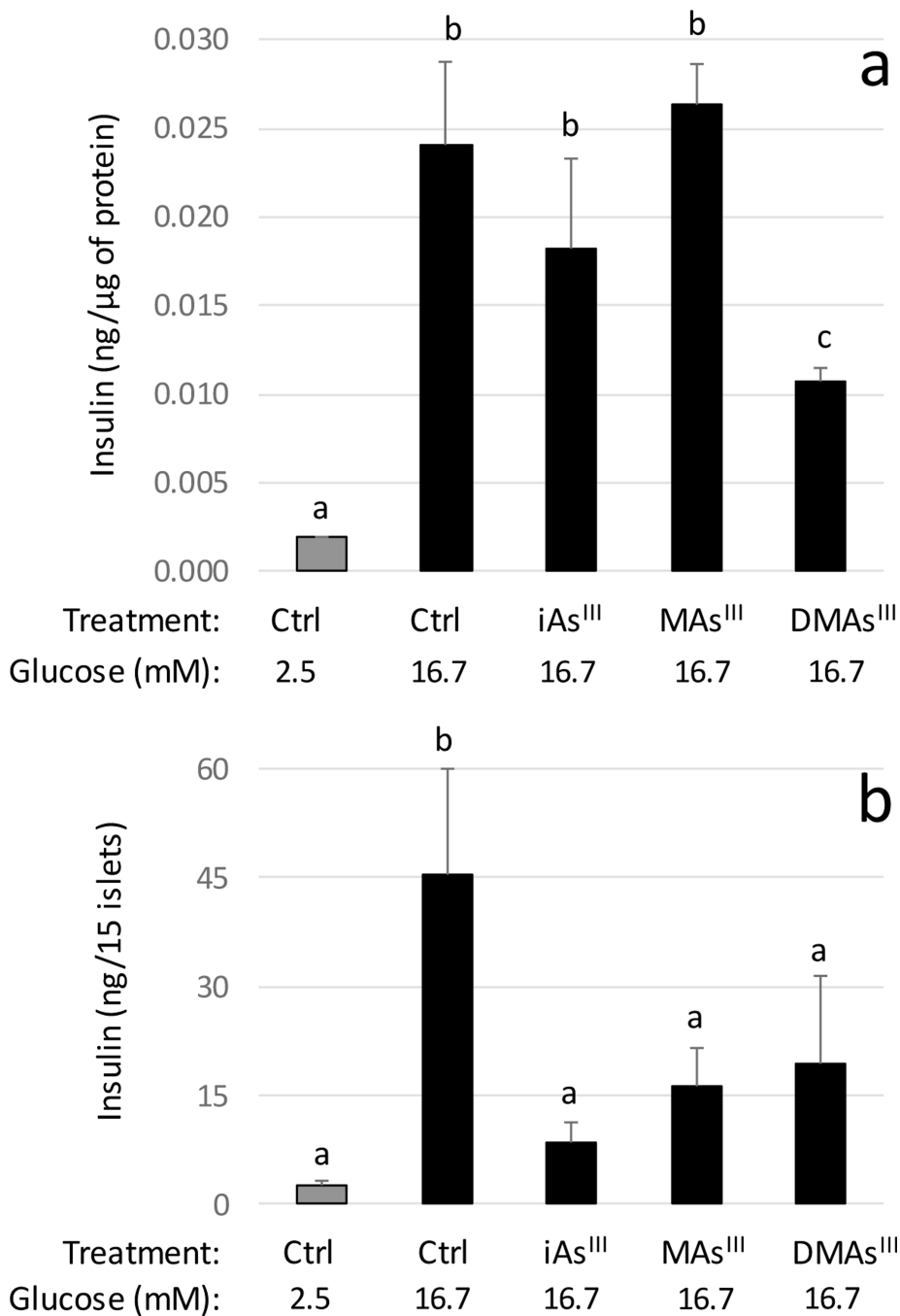


**Figure 1:** Glucose-stimulated insulin secretion by INS-1 832/13 cells (a) and isolated pancreatic islets (b) exposed to arsenicals and in unexposed controls (Ctrl) cells and islets (mean  $\pm$ SD, N=3); values labeled with different letters are significantly different ( $p < 0.05$ )

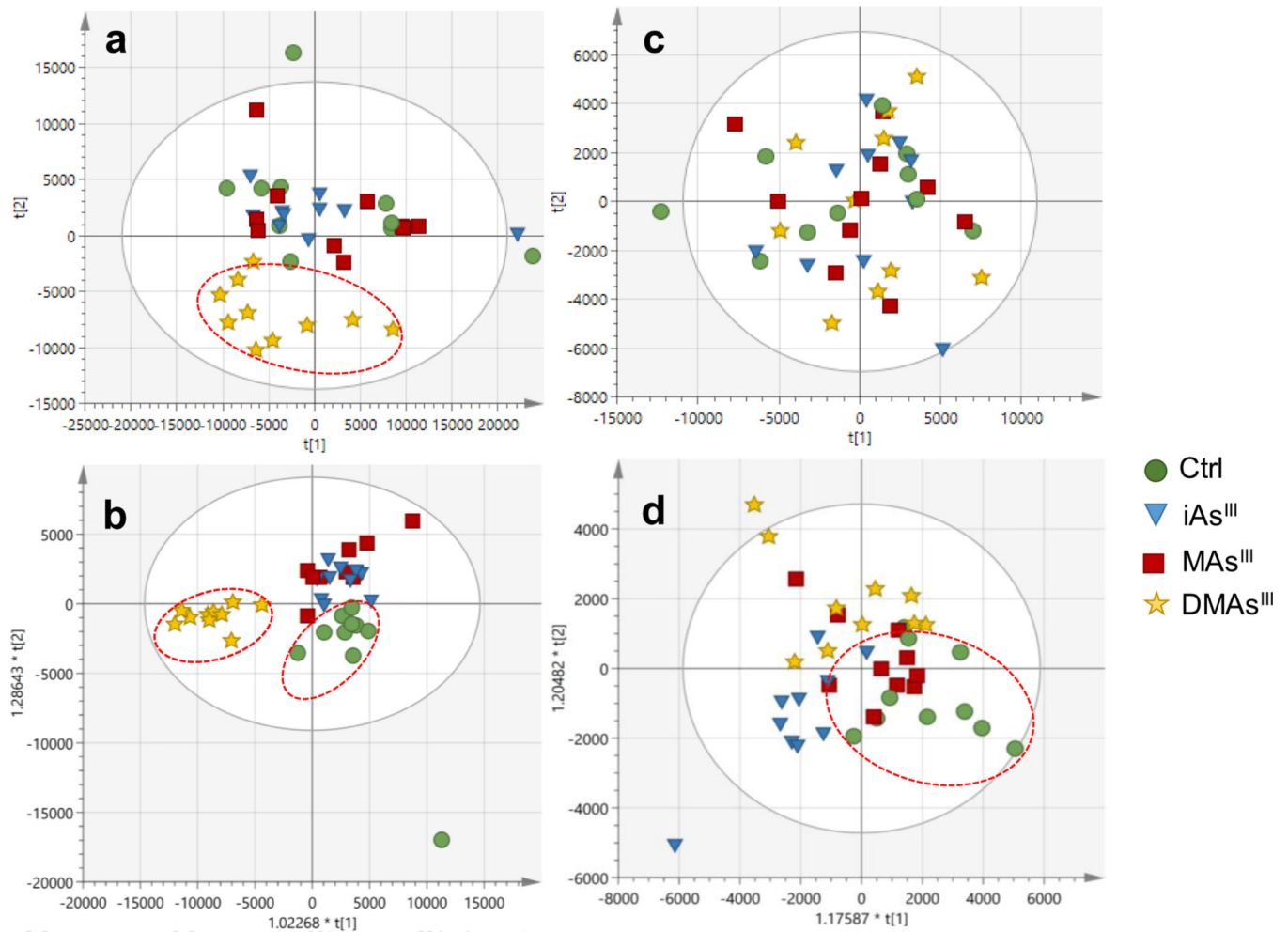


**Figure 2:** Score scatter plots of (a) principal component analysis (PCA) and (b) orthogonal projections to latent structures discriminant analysis (OPLS-DA) for INS-1 832/13 cells exposed to arsenicals and for unexposed controls (Ctrl). (c) PCA and (d) OPLS-DA for islets exposed to arsenicals and unexposed controls (Ctrl). Dotted ovals indicate samples from the same phenotypic group that clustered separately from other groups.

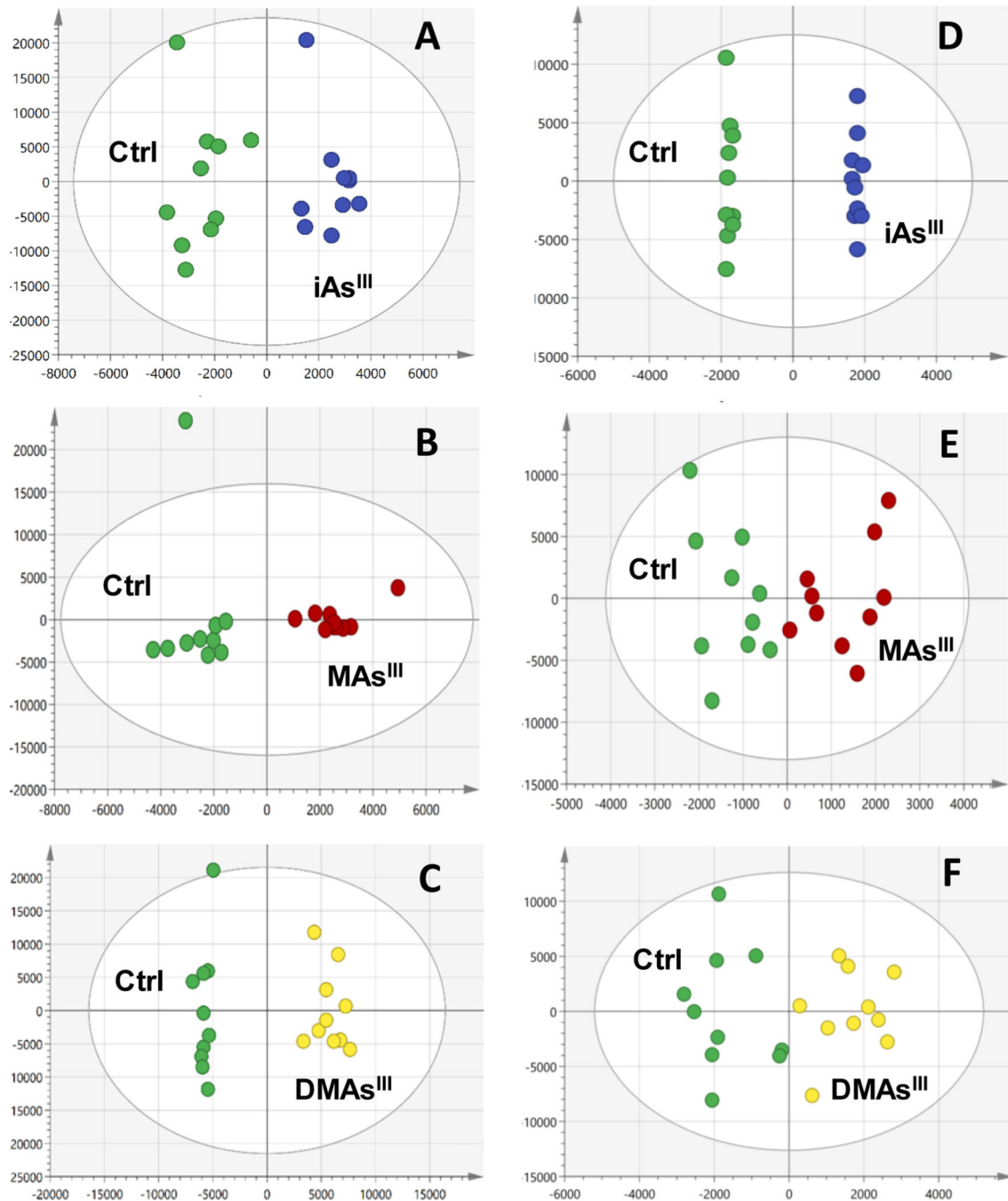


**Figure 3:** Supervised pairwise comparisons (OPLS-DA) for INS-1 832/13 cells exposed to iAs<sup>III</sup> (a), MAs<sup>III</sup> (b), and DMAs<sup>III</sup> (c) vs respective controls (Ctrl); OPLS-DA for islets exposed to iAs<sup>III</sup> (d), MAs<sup>III</sup> (e), and DMAs<sup>III</sup> (f) vs respective controls (Ctrl). Model statistics: (a), R2X(cum)=0.771, Q2(cum)=0.9; (b), R2X(cum)=0.71, Q2(cum)=0.893; (c), R2X(cum)=0.852, Q2(cum)=0.972; (d), R2X(cum)=0.718, Q2(cum)=0.628; (e), R2X(cum)=0.516, Q2(cum)= -0.91; (f), R2X(cum)=0.546, Q2(cum)= -0.221.

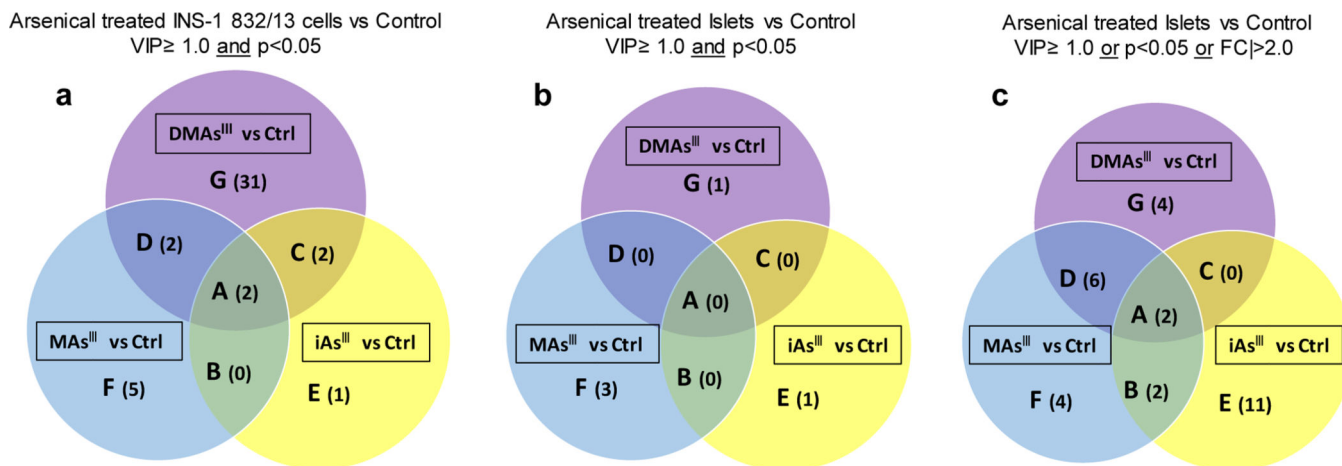
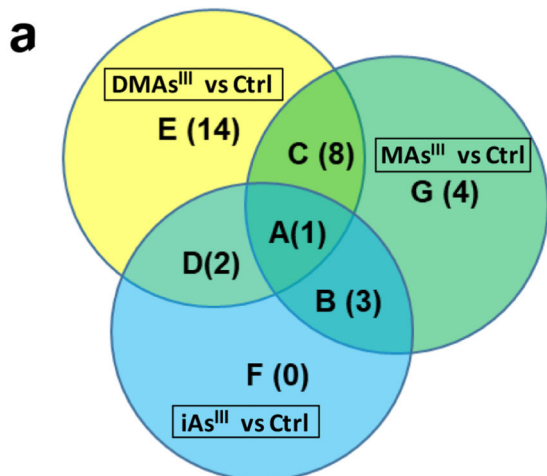


**Figure 4:**

Venn diagram of metabolites perturbed in INS-1 832/13 cells and islets exposed to arsenicals as compared to unexposed controls (Ctrl), with the cut-off VIP  $\geq 1.0$  and  $p < 0.05$  (**a**); Venn diagram of metabolites perturbed in islets exposed to arsenicals as compared to unexposed controls (Ctrl), with the cut-off VIP  $\geq 1.0$  and  $p < 0.05$  (**b**) and the cut-off VIP  $\geq 1.0$ , or  $p < 0.05$ , or  $|FC| > 2.0$  (**c**). Each section of the diagram is labeled by a capital letter (A, B, C, D, E, F, and G) and numbers of metabolites in each section are shown in parenthesis. The metabolites corresponding to each section are listed in Table 1 (for diagram **a**) and Table 2 (for diagrams **c**)



## Arsenical treated INS-1 832/13 cells vs Control



## Arsenical treated Islets vs Control

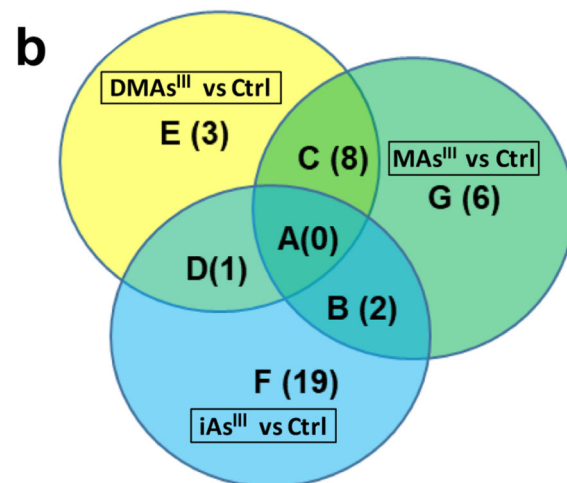


**Figure 5:**

Venn diagram of metabolic pathways perturbed in INS-1 832/13 cells (**a**) and islets (**b**) exposed to arsenicals as compared to unexposed controls (Ctrl). Pathway enrichment was conducted using Genego Metacore™, and the cut-off for pathway associations was  $p < 0.05$  (details are shown in Tables 3 and 4). Each section of the diagrams is labeled by a capital letter (A, B, C, D, E, F, and G) and numbers of pathways in each section are shown in parenthesis. The list of pathways corresponding to each section are shown in Tables 3 (for diagram **a**) and Table 4 (for diagram **b**).

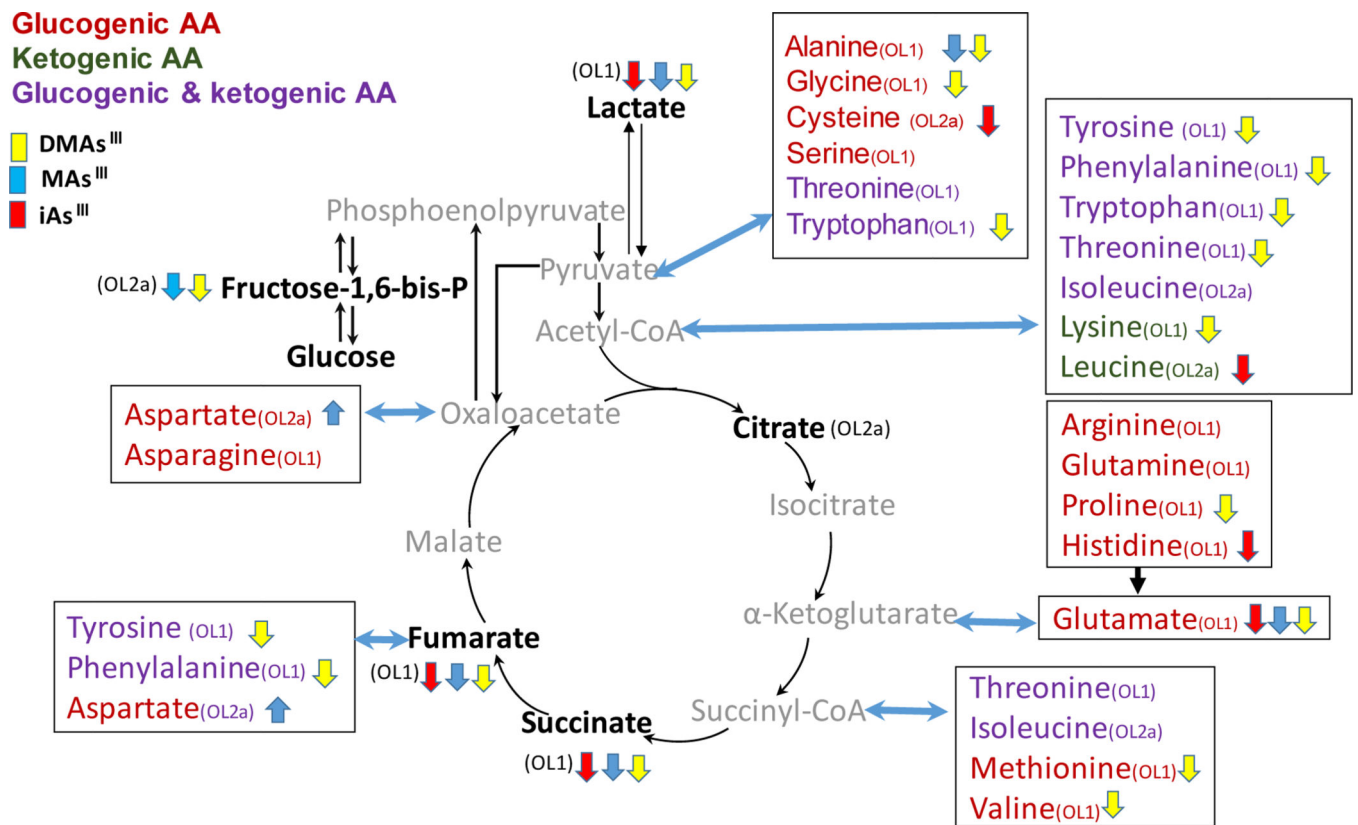


**Figure 6:** Perturbation of carbohydrate-amino acid pathways in INS-1 832/13 cells exposed to iAs<sup>III</sup>, MAs<sup>III</sup> and DMAs<sup>III</sup>. Only metabolites identified with OL-1 (RT, MS and MS/MS) or OL-2a (RT and MS) are shown. Metabolites in gray were not found in the current untargeted analysis. Metabolites labeled with ↓ were downregulated and with ↑ were upregulated by the exposure ( $p < 0.05$ ); no significant changes were found for other metabolites. Box plots of key metabolites in the pathway are shown in Supplemental Figure 1

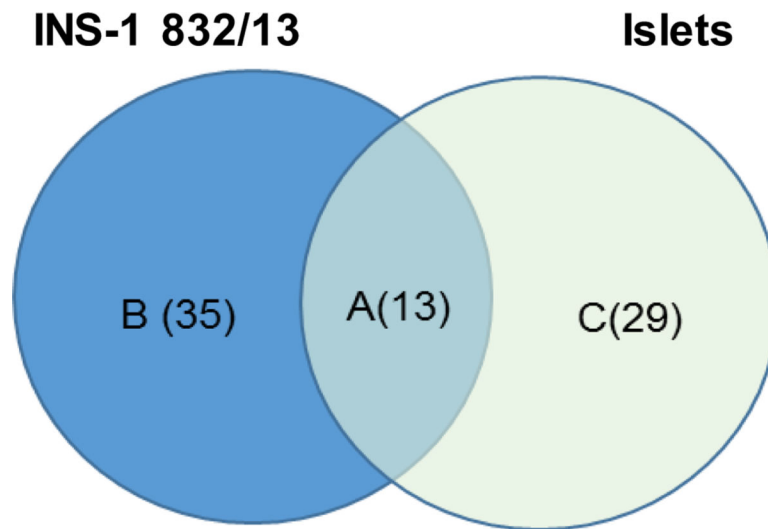


**Figure 7:** Venn diagram of metabolites perturbed in INS-1 832/13 cells and islets exposed to arsenicals. Criteria for differentiators in INS-1 832/13 cells were  $VIP \geq 1.0$  and  $p < 0.05$ ; the criteria for differentiators in islets were  $VIP \geq 1.0$  or  $p < 0.05$  or  $|FC| > 2.0$ . Metabolites in the overlap between INS-1 832/13 cells and islets (A) are listed in Table 5. Metabolites specific for INS-1 832/13 cells (B) and islets (C) sections are listed in Supplemental Table 3.

**Table 1.**

Metabolites perturbed in INS-1 832/13 cells exposed to arsenicals as compared to unexposed controls (Ctrl)

Code <sup>a</sup>	Metabolite <sup>b</sup>	Fold Change <sup>c</sup>		
		iAs <sup>III</sup> vs Ctrl	MAs <sup>III</sup> vs Ctrl	DMAs <sup>III</sup> vs Ctrl
<b>A</b>	Acetylcarnitine	-1.8	-1.6	-1.8
	Succinic acid	-1.5	-1.4	-1.7
<b>C</b>	Aminobutyric acid	-1.6		-1.6
	Nicotinamide	-1.3		-1.8
<b>D</b>	N-Methyl-L-glutamic acid		-2.5	-7.3
	Glutamic acid		-1.5	-1.6
<b>E</b>	Betaine	-1.3		
<b>F</b>	Cyclic adenosine monophosphate		2.5	
	Carnitine		1.3	
	Aspartic acid		3.6	
	Raffinose		-1.6	
	O-Phosphorylethanolamine		3.0	
<b>G</b>	4-Hydroxyphenylpyruvic acid			1.4
	Adenosine			2.7
	Azelaic acid			1.4
	Creatine			-3.0
	Cytosine			-3.0
	Guanine			-2.4
	Guanosine			-3.8
	Hypoxanthine			-2.7
	Inosine			-4.1
	Alanine			-2.2
	Glutathione reduced			-10.6
	Methionine			-1.5
	Phenylalanine			-1.5
	Proline			-1.4
	Tyrosine			-1.7
	Methylthioadenosine			-1.9
	Ornithine			-1.8
	Phosphorylcholine			-1.9
	S-Adenosyl-L-homocysteine			-3.1
	Serotonin			-1.9
Spermidine			-1.5	
Spermine			-1.7	
Suberic acid			1.4	

Code <sup>a</sup>	Metabolite <sup>b</sup>	Fold Change <sup>c</sup>		
		iAs <sup>III</sup> vs Ctrl	MAs <sup>III</sup> vs Ctrl	DMAs <sup>III</sup> vs Ctrl
	Threonine			-1.3
	Tryptophan			-1.7
	Uridine			-3.8
	Xanthine			-1.7
	5-Aminolevulinic acid			-1.3
	Cytidine			-3.6
	Valine			-1.4
	Norleucine			-1.8

<sup>a</sup>Capital letters (A-G) correspond to the area codes in Venn diagram in Fig. 4a.

<sup>b</sup>Metabolites satisfying VIP  $\geq 1.0$  and  $p < 0.05$  in pairwise comparison of the arsenical-treated and control INS-1 832/13 cells.

<sup>c</sup>Fold Change, the ratio of intensity between the arsenical treated cells vs the control cells, based on the mean, indicates the direction and magnitude of change: positive FC indicates increase compared to control and negative FC indicates decrease compared to control. Lack of FC value (gray area) indicates that the metabolite did not satisfy the above criteria.

**Table 2.**

Metabolites perturbed in pancreatic islets exposed to arsenicals as compared to unexposed controls (Ctrl)

Code <sup>a</sup>	Metabolite <sup>b</sup>	Fold Change <sup>c</sup>		
		iAs <sup>III</sup> vs Ctrl	MAs <sup>III</sup> vs Ctrl	DMAs <sup>III</sup> vs Ctrl
<b>A</b>	Suberic acid	1.0	-1.0	1.0
	Petroselinic acid	1.0	1.0	1.0
<b>B</b>	S-Adenosyl-L-methionine	-1.5	-1.9	
	Glutamic acid	-1.0	-1.0	
<b>D</b>	Citrulline		-2.0	-2.4
	Uric acid		2.3	-2.3
	Ophthalmic acid		1.5	1.4
	Acetylcarnitine		-1.2	-1.3
	Glyceryl monomyristate		1.0	-1.1
	4-Imidazoleacrylic acid		-2.2	-2.7
<b>E</b>	Sucrose	2.3		
	Azelaic acid	1.0		
	Taurine	-1.2		
	Aspartic acid	-1.1		
	Leucine	-1.0		
	Hypoxanthine	-1.0		
	Hypotaurine	3.9		
	Sorbitol	2.5		
	Orotic acid	-1.6		
	Galactose	-1.1		
Valine	-1.1			
<b>F</b>	Tyrosine		-1.1	
	Methylthioadenosine		-1.6	
	Betaine		-2.1	
	Lysine		2.4	
<b>G</b>	Glutathione reduced			-2.1
	Ornithine			-1.3
	4-Hydroxyphenylpyruvic acid			1.0
	2,6-Diaminopimelic acid			1.2

<sup>a</sup>Capital letters (A-G) correspond to the area codes in Venn diagram in Fig. 4b.<sup>b</sup>Metabolites satisfying VIP  $\geq 1.0$  or  $p < 0.05$  or  $|FC| > 2.0$  in pairwise comparison of the arsenical-treated and control islets.<sup>c</sup>Fold Change, the ratio of intensity between the arsenical treated islets vs the control islets, based on the mean, indicates the direction and magnitude of change: positive FC indicates increase compared to control and negative FC indicates decrease compared to control. Lack of FC value (gray area) indicates that the metabolite did not satisfy the above criteria.



**Table 3.**

Enriched metabolic pathways perturbed in INS-1 832/13 cells exposed to arsenicals

Code <sup>a</sup>	Treatment	Enriched Pathways	Direction of change <sup>b</sup>	-log (p-value) <sup>c</sup>	FDR <sup>d</sup>	
<b>A</b>	iAs <sup>III</sup>		↓	2.1	1.4E-02	
	MAs <sup>III</sup>	D-glucuronic acid pathway	↓	6.1	2.1E-05	
	DMAs <sup>III</sup>		↓	3.1	1.7E-03	
<b>B</b>	iAs <sup>III</sup>		↓	3.4	3.1E-03 03	
	MAs <sup>III</sup>	(L)-carnitine pathway	↑ <sup>e</sup>	2.4	7.9E-03	
	MAs <sup>III</sup>		↓ <sup>f</sup>	2.9	5.9E-03	
	iAs <sup>III</sup> MAs <sup>III</sup>	Carbohydrate metabolism, Propionate metabolism and transport	↓ ↓	3.1 2.5	3.1E-03 8.2E-03	
	iAs <sup>III</sup> MAs <sup>III</sup>	Carbohydrate metabolism, TCA and tricarboxylic acid transport	↓ ↓	3.3 2.7	3.1E-03 7.1E-03	
<b>C</b>	MAs <sup>III</sup> DMAs <sup>III</sup>	(L)-phenylalanine pathways and transport	↓ ↓	2.6 8.4	8.2E-03 5.9E-08	
	MAs <sup>III</sup> DMAs <sup>III</sup>	Amino acid metabolism: Arginine metabolism and transport	↓ ↓	1.5 4.2	6.9E-02 2.4E-04	
	MAs <sup>III</sup> DMAs <sup>III</sup>	Amino acid metabolism: Asparagine, Aspartic acid metabolism and transport	↓ ↓	3.9 2.4	7.1E-04 8.0E-03	
	MAs <sup>III</sup> DMAs <sup>III</sup>	Glutamic acid pathway	↓ ↓	5.4 8.8	4.6E-05 5.9E-08	
	MAs <sup>III</sup> DMAs <sup>III</sup>	Glutamic acid pathways and transport	↓ ↓	4.8 7.3	1.1E-04 4.0E-07	
	MAs <sup>III</sup> DMAs <sup>III</sup>	L-glutamate pathways and transport	↓ ↓	4.9 7.7	1.0E-04 2.3E-07	
	MAs <sup>III</sup> DMAs <sup>III</sup>	L-citrulline pathway	↓ ↓	1.7 4.9	4.8E-02 5.8E-05	
	MAs <sup>III</sup> DMAs <sup>III</sup>	L-ornithine pathways and transport	↓ ↓	2.5 5.8	9.1E-03 8.2E-06	
	<b>D</b>	iAs <sup>III</sup> DMAs <sup>III</sup>	Amino acid metabolism: Ala, Ser, Cys, Met, His, Pro, Gly, Glu, Gln metabolism and transport	↓ ↓	2.5 7.0	7.9E-03 6.5E-07
		iAs <sup>III</sup> DMAs <sup>III</sup>	Lipid metabolism: Glycosphingolipid metabolism	↓ ↓	2.5 7.0	7.9E-03 6.5E-07
	<b>E</b>	DMAs <sup>III</sup>	(L)-alanine pathways and transport	↓	3.5	8.7E-04
		DMAs <sup>III</sup>	(L)-proline pathways and transport	↓	8.4	5.9E-08
		DMAs <sup>III</sup>	(L)-threonine pathways and transport	↓	4.7	7.6E-05
DMAs <sup>III</sup>		(L)-valine pathways and transport	↑	2.6	1.0E-02	
DMAs <sup>III</sup>		1-icosatrienoyl-sn-glycero-3-phosphocholine pathway	↑	2.4	1.0E-02	

Code <sup>a</sup>	Treatment	Enriched Pathways	Direction of change <sup>b</sup>	-log (p-value) <sup>c</sup>	FDR <sup>d</sup>
	DMA <sub>s</sub> <sup>III</sup>	Amino acid metabolism: Ala, Gly, Cys metabolism and transport	↓	4.1	2.7E-04
	DMA <sub>s</sub> <sup>III</sup>	Amino acid metabolism: Try metabolism and transport	↓	4.0	3.3E-04
	DMA <sub>s</sub> <sup>III</sup>	Amino acid metabolism: Try, Phe, Met metabolism	↓	1.9	2.1E-02
	DMA <sub>s</sub> <sup>III</sup>	Amino acid metabolism: Try, Phe, Tyr, Met metabolism and transport	↓	3.3	1.4E-03
	DMA <sub>s</sub> <sup>III</sup>	Glycine pathways and transport	↓	2.4	8.2E-03
	DMA <sub>s</sub> <sup>III</sup>	L-serine pathways and transport	↓	1.4	6.7E-02
	DMA <sub>s</sub> <sup>III</sup>	Methionine pathways and transport	↓	3.2	1.6E-03
	DMA <sub>s</sub> <sup>III</sup>	Tyrosine pathway	↓	5.8	7.6E-06
	DMA <sub>s</sub> <sup>III</sup>	Vitamin, mediator and cofactor metabolism: Nitric	↓	2.9	2.8E-03
	MA <sub>s</sub> <sup>III</sup>	O-hexadecanoyl-(L)-carnitine pathway	↑	2.7	6.1E-03
<b>G</b>	MA <sub>s</sub> <sup>III</sup>	Amino acid metabolism: (L)-carnitine metabolism	↑	5.1	9.2E-05
	MA <sub>s</sub> <sup>III</sup>	Decanoylcarnitine pathway	↑	4.2	2.7E-04
	MA <sub>s</sub> <sup>III</sup>	Lauroylcarnitine pathway	↑	4.1	2.7E-04

<sup>a</sup>Capital letters (A-G) correspond to the area codes shown in Venn diagram in Fig. 5a.

<sup>b</sup>↑, up-regulation by arsenical treatment vs control; ↓, down-regulation by arsenical treatment vs control.

<sup>c</sup>p-value was generated from the hypergeometric test in Metacore; it indicates the significance of enrichment of metabolites in pathway mapping.

<sup>d</sup>FDR, false discovery rate.

<sup>e</sup>carnitine pathway related to L-Carnitine cytoplasm, L-Carnitine mitochondrial matrix;

<sup>f</sup>carnitine pathway related to L-Acetylcarnitine extracellular region, L-Acetylcarnitine cytosol, L-Acetylcarnitine cytoplasm.

**Table 4.**

Enriched metabolic pathways perturbed in pancreatic islets exposed to arsenicals

Code <sup>a</sup>	Treatment	Enriched Pathways	Direction of change <sup>b</sup>	-log (p-value) <sup>c</sup>	FDR <sup>d</sup>
<b>B</b>	iAs <sup>III</sup>	Glutamic acid pathways and transport	↓	5.0	2.6E-04
	MA <sup>s</sup> III		↓	1.4	7.8E-02
	iAs <sup>III</sup>	L-glutamate pathways and transport	↓	1.4	6.0E-02
	MA <sup>s</sup> III		↓	1.4	7.4E-02
<b>C</b>	DMA <sup>s</sup> III	(L)-carnitine pathway	↓	2.8	5.2E-03
	MA <sup>s</sup> III		↓	3.0	1.1E-02
	DMA <sup>s</sup> III	(L)-proline pathways and transport	↓	3.7	6.9E-04
	MA <sup>s</sup> III		↑	2.8	2.5E-03
	DMA <sup>s</sup> III	Amino acid metabolism: Arginine metabolism and transport	↓	3.7	6.9E-04
	MA <sup>s</sup> III		↓	1.6	6.3E-02
	DMA <sup>s</sup> III	Amino acid metabolism: Try, Phe, Tyr, Met metabolism and transport	↑	1.5	3.3E-02
	MA <sup>s</sup> III		↓	1.3	8.4E-02
	DMA <sup>s</sup> III	L-citrulline pathway	↓	5.6	2.1E-05
	MA <sup>s</sup> III		↓	1.8	6.3E-02
	DMA <sup>s</sup> III	Lipid metabolism: Glycosphingolipid metabolism	↓	1.8	3.2E-02
	MA <sup>s</sup> III		↓	2.1	4.9E-02
	DMA <sup>s</sup> III	Vitamin, mediator and cofactor metabolism: Nitric oxide biosynthesis and transport	↓	10.7	3.7E-10
	MA <sup>s</sup> III		↓	3.7	4.2E-03
<b>D</b>	DMA <sup>s</sup>	Amino acid metabolism: Ala, Ser, Cys, Met, His, Pro, Gly, Glu, Gln metabolism and transport	↓	1.8	3.2E-02
	MA <sup>s</sup> III		↓	2.1	4.9E-02
<b>E</b>	DMA <sup>s</sup> III	(S)-citrulline pathway	↓	4.9	8.4E-05
	iAs <sup>III</sup>	L-ornithine pathways and transport	↓	2.6	1.4E-02
	DMA <sup>s</sup> III	Amino acid metabolism: Try, Phe, Meth metabolism	↑	1.7	3.6E-02
<b>F</b>	DMA <sup>s</sup> III	Tyrosine pathway	↑	1.5	3.3E-02
	iAs <sup>III</sup>	Carbohydrate metabolism: Galactose metabolism and transport	↑ <sup>e</sup>	1.4	5.8E-02
			↓ <sup>f</sup>	1.6	5.6E-02
	iAs <sup>III</sup>	Carbohydrate metabolism: Sucrose metabolism and transport	↑ <sup>g</sup>	1.3	5.8E-02
			↓ <sup>h</sup>	1.6	5.7E-02
	iAs <sup>III</sup>	(L)-leucine pathways and transport	↓	3.1	1.1E-02
	iAs <sup>III</sup>	(L)-valine pathways and transport	↓	2.9	1.1E-02
	iAs <sup>III</sup>	1-acyl-glycerol 3-phosphocholine pathway	↓	1.7	5.1E-02
iAs <sup>III</sup>	1-docosahexaenoyl-glycerol_3-phosphocholine pathway	↓	1.4	6.0E-02	

Code <sup>a</sup>	Treatment	Enriched Pathways	Direction of change <sup>b</sup>	-log (p-value) <sup>c</sup>	FDR <sup>d</sup>
	iAs <sup>III</sup>	1-icosatrienoyl-sn-glycero-3-phosphocholine pathway	↓	1.5	6.0E-02
	iAs <sup>III</sup>	1-oleoyl-sn-glycero-3-phosphocholine pathway	↓	1.5	6.0E-02
	iAs <sup>III</sup>	1-palmitoyl-sn-glycero-3-phosphocholine pathway	↓	1.8	5.1E-02
	iAs <sup>III</sup>	2-arachidonoyl-glycerol_3-phosphocholine pathway	↓	1.4	6.3E-02
	iAs <sup>III</sup>	Amino acid metabolism: Ala, Gly, Cys metabolism and transport	↓	2.7	1.4E-02
	iAs <sup>III</sup>	Amino acid metabolism: Branched-chain amino acid metabolism	↓	1.6	5.6E-02
	iAs <sup>III</sup>	Carbohydrate metabolism: Fructose metabolism and transport	↑	3.3	2.4E-03
	iAs <sup>III</sup>	GalNAcβ1-3Gal pathway	↑	1.4	5.8E-02
	iAs <sup>III</sup>	Glucosylceramide pathways and transport	↓	1.8	5.1E-02
	iAs <sup>III</sup>	Sucrose pathway	↑	3.4	2.4E-03
	iAs <sup>III</sup>	Vitamin, mediator and cofactor metabolism CoA biosynthesis and transport	↓	1.8	5.1E-02
	MA <sup>sIII</sup>	(L)-lysine pathways and transport	↑	4.9	3.6E-05
	MA <sup>sIII</sup>	(L)-phenylalanine pathways and transport	↓	1.6	6.3E-02
<b>G</b>	MA <sup>sIII</sup>	Amino acid metabolism: Ala, Gly, Cys metabolism and transport	↓	1.5	6.3E-02
	MA <sup>sIII</sup>	Amino acid metabolism: Lysine metabolism and transport	↑	1.5	3.0E-02
	MA <sup>sIII</sup>	Glutamic acid pathway	↓	1.6	6.3E-02
	MA <sup>sIII</sup>	Methionine pathways and transport	↓	1.5	6.3E-02

<sup>a</sup>Capital letters (A-G) correspond to the area codes shown in Venn diagram in Fig. 5b.

<sup>b</sup>↑, up-regulation by arsenical treatment vs control; ↓, down-regulation by arsenical treatment vs control.

<sup>c</sup>p-value was generated from the hypergeometric test in Metacore; it indicates the significance of enrichment of metabolites in pathway mapping.

<sup>d</sup>FDR, false discovery rate.

<sup>e</sup>pathways associated with D-Sorbitol intracellular;

<sup>f</sup>pathways associated with D-Galactose intracellular, D-Galactose extracellular region;

<sup>g</sup>pathways associated D-Sucrose extracellular region;

<sup>h</sup>D-Galactose intracellular, D-Galactose extracellular region.

**Table 5.**

Metabolites perturbed in both INS-1 832/13 cells and pancreatic islets exposed to arsenicals as compared to the corresponding unexposed controls (Ctrl)

Metabolites <sup>a</sup>	FC in INS-1 832/13 Cells <sup>b</sup>			FC in Islets <sup>b</sup>		
	iAs <sup>III</sup> vs Ctrl	MAs <sup>III</sup> vs Ctrl	DMAs <sup>III</sup> vs Ctrl	iAs <sup>III</sup> vs Ctrl	MAs <sup>III</sup> vs Ctrl	DMAs <sup>III</sup> vs Ctrl
Acetylcarnitine	-1.8	-1.6	-1.8		-1.2	-1.3
Glutamic acid		-1.5	-1.6	-1.0		
Aspartic acid		3.6		-1.1		
Glutathione reduced			-10.6			-2.1
Hypoxanthine			-2.7	-1.0		
Methylthioadenosine			-1.9		-1.6	
Leucine			-1.8	-1.0		
Ornithine			-1.8			-1.3
Valine			-1.4	-1.1		
4-Hydroxyphenylpyruvic acid			1.4			1.0
Azelaic acid			1.4	1.0		
Suberic acid			1.4	1.0	-1.0	1.0
Betaine	-1.3				-2.1	

<sup>a</sup>The metabolites correspond to section A of Venn diagram in Fig. 7. The criteria for identification of differentially altered metabolites were VIP 1.0 and  $p < 0.05$  for INS-1 832/13 cells and VIP 1.0 or  $p < 0.05$  or  $|\text{FC}| > 2.0$  for the islets.

<sup>b</sup>FC, fold change, the ratio of intensity between the arsenical-treated vs control INS-1 832/13 cells or islets, based on the mean, indicates the direction and magnitude of the metabolites impacted by arsenical treatments; positive FC indicates increase compared to control and negative FC indicates decrease compared to control. Lack of FC value (gray area) indicates that the metabolite did not satisfy the above criteria.